

Moral Dilemma Judgment Revisited: A Loreta Analysis

Armando Freitas da Rocha¹, Fábio Theoto Rocha^{1,2}, Eduardo Massad³

¹Research on Natural and Artificial Intelligence (RANI), Jundiaí, Brazil

²Instituto de Pesquisas em Teoria da Informação (IPTI), Aracajú, Brazil

³Faculdade de Medicina da Universidade de São Paulo (FMUSP), São Paulo, Brazil

Email: armando@enscer.com.br; fabio@enscer.com.br; edmassad@usp.br

Received October 15, 2013; revised November 25, 2013; accepted December 12, 2013

Copyright © 2013 Armando Freitas da Rocha *et al.* This is an open access article distributed under the Creative Commons Attribution License, which permits unrestricted use, distribution, and reproduction in any medium, provided the original work is properly cited.

ABSTRACT

Background: Recent neuroscience investigations on moral judgment have provided useful information about how brain processes such complex decision making. All these studies carried out so far were fMRI investigations and therefore were constrained by the poor temporal resolution of this technique. Recent advances in electroencephalography (EEG) analysis provided by Low Resolution Tomography (Loreta), Principal Component (PCA), Correlation and Regression Analysis improved EEG spatial resolution and made EEG a very useful technique in decision-making studies. **Methods:** Here, we reinvestigate previous fMRI study of personal (PD) and impersonal (ID) moral dilemma judgment, taking profit of these new EEG analysis improvements. **Results:** PCA analysis disclosed three different patterns of brain activity associated with dilemma judgment. These patterns are proposed to disclose the neural circuits involved in benefit and risk evaluation, calculating intention to act and controlling decision-making. Regression analysis showed that activity at some cortical areas favors action implementation by increasing intention to act, while activity at some other areas opposes it by decreasing intention to act. **Comparison with Existing Methods:** Compared to the previous fMRI results, Loreta and PCA revealed a much greater number of cortical areas involved in dilemma judgment, whose temporal and spatial distribution were different for ID compared to PD. The present paper suggests that whenever final temporal details of the decision making process are desired, EEG becomes the tool of choice as compared with fMRI. **Conclusions:** The presented results are discussed from the utilitarian point of view that proposes adequacy of human action being dependent upon how much pleasure and fear/pain they are associated.

Keywords: Loreta; EEG; PCA; Regression Analysis; Brain Mapping

1. Introduction

Recent development of new techniques for studying the human brain has brought moral and ethical discussions to the realm of neuroscience investigations [1-4].

Greene *et al.* [2] were among the first to use fMRI to study moral dilemma judgment and in other two papers [3,4] they explore the cerebral areas involved in judgment of *personal* (PD) and *impersonal* (ID) like the trolley dilemma (as ID example) and the foot bridge dilemma (as PD example):

The trolley dilemma: (D) A runaway trolley is headed for five people who will be killed if it proceeds on its present course. **(A)** The only way to save them is to hit a switch that will turn the trolley onto an alternate set of tracks where it will kill one person instead of five. **(J)** Is it appropriate to switch the tracks?

The foot bridge dilemma: (D) Similar to the trolley dilemma, the trolley is on a path that will kill five people. **(A)** The five people could be saved if you push a stranger in front of the trolley; however, the stranger would be killed. **(J)** Is it appropriate to push the stranger?

Such dilemmas have the following structure:

- proposition **D** describes a situation that implies a social loss (dead) of a given value (5 people);
- proposition **A** describes an action to avoid the social loss but at a personal risk of a given intensity (hitting a switch or pushing a stranger), and
- a question **(J)** asks the individual to decide whether **A** is appropriate in the context introduced by **D**.

Although the two dilemmas have the same logical structure, the judgments about these two dilemmas are totally different because they imply a similar benefit

(avoid a given social loss) but at two different personal risks (hitting a switch = low risk, or pushing a stranger = higher risk). Decision about saving 5 as the cost of killing 1 is taken by 50% of individuals for **ID** dilemma and only 30% of them for **PD** judgment. As action adequacy decreases as personal risk increases [1], these reported responses are the expected ones.

However, Greene *et al.* [2,3], assumed that their fMRI results support the claim that “*a theory moral judgment according to which both “cognitive” and “emotional processes” play crucial and sometimes mutually competitive roles*”. They assume that brain regions like dorsolateral prefrontal and anterior cingulate cortices (areas associated with abstract and cognitive reasoning) are recruited to inhibit activity in emotion-related brain regions (e.g., posterior cingulate cortex and insula). These latter are involved in the solution of difficult personal moral dilemmas, in which utilitarian values require personal moral violations. These conclusions are in opposition to those of Rocha *et al.*[1] assuming that cognition and emotion play complementary roles in any kind of decision making, which has to take into consideration both the associated benefit and risk. As a matter of fact, only recently Shenhav and Greene [4] used regression analysis to correlate activity in previously chosen regions of interest and regressors like intended moral value [4] that is to study the dependence of dilemma judgment upon the expected benefit but not risk. This is in contrast with the concept of *utility* of an action as defined by Bentham [5], who was among the first to propose the *theory of utilitarianism*. According to him, utility is dependent on both *pleasure* (benefit) and *pain* (risk) as estimated by the individual or the community.

Greene *et al.* [3] presented each dilemma as a text through a series of three screens, the first two describing **D** and **A**, and the last posing the question **J**. Subjects read at their own pace, pressing a button to advance from the first to the second screen and from the second to the third screen. However, because of the well-known fMRI time resolution constraints, these authors [3] used a floating window of eight images surrounding (four prior to, one during, and three following) the time of response, when individuals pressed one of two buttons (“appropriate” or “inappropriate”) according to their dilemma judgment. They included three post-response images in order to allow for the lag in BOLD response (typically peaking de following 3-5s an eliciting neural response). Therefore, their fMRI analysis involved a global time widow of 16s long that did not discriminate among the distinct cerebral processing required by **D**, **A** and **J** phases of dilemma judgment. In all their papers [2-4], the authors described around 30 different cortical areas as involved in dilemma judgment.

LORETA (Low Resolution Tomography) uses measurements of scalp electric potential differences (EEG) or

extracranial magnetic fields (MEG) to find the 3D distribution of the generating electric neuronal activity with exact zero error localization to point-test sources [6]. LORETA has the capability of identifying 6430 voxels at 5 mm spatial resolution in cortical gray matter and hippocampus

(<http://www.uzh.ch/keyinst/NewLORETA/sLORETA/sLORETA.htm>). This technique has been widely used (e.g., [7-12]) to study the neural correlates of cognition, because it combines the portability and high temporal resolution of EEG technique with a reasonable spatial identification of the cortical signal electrical sources s_l . Principal Component Analysis (PCA) of the amount of information $H(e_i)$, provided by electrode e_i (see methods) about the identified LORETA sources (**ILS**), was used to study how these sources interact to solve a cognitive task [13-15].

Because the understanding of brain functioning supporting dilemma judgment requires the analysis of the different tasks involved in **D**, **A** and **J** phases, we decide to reinvestigate brain activity associated with the judgment of the same dilemmas as in [3], but now using EEG and LORETA analysis to disclose the distinct **ILS**s associated the analysis carried out during **D**, **A** and **J** phases. This is done to take profit of the high temporal EEG resolution to study the complexity of the interactions between the different neural circuits involved in moral judgment. Because of the high temporal EEG resolution we expect to identify, in contrast with the previous authors, a high number of cortical areas involved with dilemma judgment.

The main hypotheses of the present paper are:

- 1) the high temporal EEG resolution makes this technique to be a necessary tool for the study of complex cognitive tasks as dilemma judgment;
- 2) Loreta analysis will identify a high number of cortical sites s_l related to this task,
- 3) $H(e_i)$ PCA analysis will identify the most important patterns of temporal and spatial correlation between these s_l .

If the above hypotheses are validated, then

- 4) dilemma judgment has to be the result of the enrollment of many different neural circuits in charge to evaluate benefits and risks associated with **D** and **A** and using these evaluations to calculate the adequacy of action proposed in **A** as its solution and the willingness of implementing this action.

2. Materials and Methods

Eleven female and twelve male adults (the mean age was 27 y and 3 mo) volunteered to solve 30 dilemmas, which were previously used by [3], while his/her EEG was registered with 20 electrodes placed according to the 10/20 system [impedance smaller than 10 kohm; low bandpass filter (50 Hz); a sampling rate of 256 Hz and 10 bits res-

olution, ear lobe reference). The dilemmas were translated to Portuguese by one of the authors having a degree in Linguistics.

Two networked personal computers were used in the present study: one for the EEG recording and the other for sequentially displaying propositions **D** and **A** and prompting for decision in **J**. The volunteers were allowed to take as much time as they needed to read **D** and **A**, and to decide about dilemma solution in **J**. We recorded the beginning times t_F , t_A , t_D of each one of these experimental epochs **D**, **A** and **J**, respectively and the time t_S the decision was made. The mean reading times Δ_D and Δ_A during the experimental epoch **D** and **A** and the mean deciding time Δ_J were calculated by the following equations and used to define the 3 different EEG epochs to be analyzed, corresponding to the experimental epochs **D**, **A** and **J**:

$$\begin{aligned}\Delta_D &= 1/n \sum_{i=1}^n (t_A - t_F) \\ \Delta_A &= 1/n \sum_{i=1}^n (t_D - t_A) \text{ and} \\ \Delta_F &= 1/n \sum_{i=1}^n (t_S - t_D)\end{aligned}\quad (1)$$

where n is the number of volunteers. The three different selected EEG epochs (**D**, **A** and **F**) were composed by the electrical activity recorded for periods of time $t_F - \Delta$, $t_A - \Delta$ and $t_S - \Delta$, respectively. These time epochs were defined in order to allow us to study the brain activity associated with the evaluation of the benefit promised in **D**, the action difficulty and risk as described in **A** and action utility or adequateness as calculated in **F**. The value Δ was set as four seconds. A total of 75 EEG epochs (30 dilemma multiplied by the 3 (**D**, **A** and **F**) experimental epochs) was selected for each volunteer, and a total of 1725 EEG epochs were initially considered for analysis. These EEG samples were visually inspected for artifacts before and those records (e.g., when eye movements could compromise the results of the regression analysis) were discarded, resulting in 1656 EEG epochs being actually used in this study.

Low Resolution Electromagnetic Tomography (Loreta) developed by [6] was used to localize the possible EEG source generators S_i associated with the cognitive tasks involved in **D**, **A**, and **F** epochs. For this purpose, the recorded data corresponding **D**, **A**, and **F** epochs associated with each **ID** or **PD**, were averaged for each electrode and all volunteers into different files averaged (**D**, **A**, and **F**). Each of these files was composed, therefore, by the corresponding EEG averages calculated for each of the 20 electrodes used to record the associated electrical activity to each experimental epoch **D**, **A**, and **F** of all **ID**s or **PD**s. In addition, two files, labeled **ID** and **PD**, were calculated by averaging each electrode in the averaged files **D**, **A**, and **F** for each dilemma type. Grand average files (**Gx**, $X = \mathbf{D}, \mathbf{A}, \mathbf{F}, \mathbf{ID}$ or **PD**) were calcu-

lated by averaging data associated with all 20 electrodes in each file **X**. The corresponding Z score was calculated for each **Gx** in order to determine the EEG times that were statically significant for Loreta Analysis. Only those EEG moments with Z score greater than 1.961 (5% significance level) were selected for this analysis. Only the areas showing the best matching for each selected EEG moment was assumed as possible EEG source generators s_i .

The amount of information $H(e_i)$ provided by electrode e_i was calculated to summarize information by electrodes e_i about the identified sources S_i . Following [14] and [15], the *informational equivalence* $H(r_i, r_j)$, was calculated as

$$H(r_{i,j}) = E(I(r_{i,j})) = K \cdot r_{i,j} \cdot (1 - r_{i,j}) \quad (2)$$

such that for $K = 4$, $H(r_{i,j}) = 1$ for $r_{i,j} = 0.5$ and $H(r_{i,j}) = 0$ for either $r_{i,j} = 1$ or $r_{i,j} = 0$.

Now, given

$$\bar{r}_i = \frac{\sum_{j=1}^{19} r_{i,j}}{19} \quad (3)$$

the *informational equivalence* measured by \bar{r}_i was calculated as

$$H(\bar{r}_i) = K \cdot \bar{r}_i (1 - \bar{r}_i) \quad (4)$$

and it quantifies the information provided by $d_i(t)$ concerning that provided by all other $d_i(t)$.

In this context, the quantity of information provided by $d_i(t)$ recorded by e_i about the sources s_i involved in solving the present reading and listening tasks was calculated as

$$H(e_i) = \frac{\sum_{j=1}^{19} [H(\bar{r}_i) - H(r_{i,j})]}{19} \quad (5)$$

such that

1) if $r_{i,j} = k$ for all all e_j then $\bar{r}_i = k$, $H(r_{i,j}) = H(\bar{r}_i)$ for all e_j , and consequently $H(e_i) = 0$. This indicates that $d_i(t)$ e_i does not provide any additional information about the sources s_i , and

2) if $r_{i,j} = 0$ for half of e_j and $r_{i,j} = 1$ for the other half, then $\bar{r}_i = 0.5$, $H(\bar{r}_i) = 1$, $H(r_{i,j}) = 0$ for all e_j , and consequently $H(e_i)$ is maximum and equal to 1. This indicates that $d_i(t)$ e_i discriminates to two different groups of electrodes providing information about distinct groups of sources s_i . However, as discussed above, the required restrictions upon $r_{i,j}$ are expected to be rare occasion. Finally,

3) for all other conditions $0 < H(e_i) < 1$ and quantifies the information provided by $d_i(t)$ about the sources s_i .

PCA was used to study the covariation of $H(e_i)$ calculated for **L**, **R**, **V_L**, **V_R** and **D** epochs. The results revealed that four factors F_j ($j=1,2,3$) accounted for more than 80% of $H(e_i)$ covariation of $H(e_i)$ for each of these analyses. The resulting eigenvalues for all of the factors were greater than 1.3. Factorial brain mappings (**Figure 1**) were constructed to describe the results of the factorial analyses. These brain mappings were constructed by taking into account the significant (greater than 0.60) loading values $f_j(e_i)$ of each electrode e_i on each factor F_j .

Logistic regression analysis was used to study the possible correlation between dilemma judgment ($J = \text{Yes} = 1, J = \text{No} = 0$) $H(e_i)$ assuming gender was assumed as a dummy variable in the model [16]:

$$J = a + \beta_i H(e_i) + \beta_{21} \Delta + \beta_{22} S^2 + \beta_{23} \text{Max}(S) + \delta_i G H(e_i) + \delta_{23} G \Delta + \delta_{24} G S^2 + \chi \delta_{25} G \text{max}(S) \quad (6)$$

G is the dummy having value 1 for female and 0 for male. In this context, the coefficients δ_i provide a measure of female impact on J calculated by equation 5. δ_i helps to determine whether there is a discrimination in J between men and women. If $\delta_i < 0$ (negative coefficient), then the same judgment J by woman requires $H(e_i)$ greater than in case of man. On the other hand, if $\delta_i > 0$ (positive coefficient), then the same judgment J by woman requires $H(e_i)$ smaller than in case of man. Note that the coefficients δ_i attached to the dummy variable G are differential intercept coefficients in contrast to the angular coefficients β_i .

3. Results

We first describe the results obtained with LORETA analysis of data contained in the files **ID** and **PD** because this analysis is more similar to that of Greene's fMRI analysis, once these files were constructed by averaging all (**D**, **A** and **J**) EEG epochs for either **ID** or **PD**, and Greene's analysis involved 16s of acquired data obtained with floating windows of eight images the time of response.

A total of 396 possible sources s_i of the averaged EEG in **ID** or **PD** were identified in 77 different cortical locations (l_i) because their calculated Z score was greater than 2. The frequencies which s_i were identified at these locations are shown in **Figure 2**. Of these 77 locations, 11 and 10 sites identified as unique and distinctive sources (**DS** in **Figure 2**) for either **ID** or **PD**, respectively. The remaining 66 and 67 locations were common to both types of dilemmas (**CS** in **Figure 2**).

Figure 3 shows the spatial and temporal distribution of the activation of these s_i and it clearly shows that both **ID** and **PD** judgment were associated with the activation of neurons widely distributed over the entire cor-

tex in a very complex temporal dynamics. The Pearson's correlation coefficient for the two series **ID** and **PD** of s_i activation was 0.01 showing that although most s_i were common to both judgment they were activated in very distinctive ways. In addition, many of these s_i were also activated at different locations during **ID** and **PD** judgment as show in **Figure 3**—mappings **ID**vs**PD**. Cuneus (BA 18 and 19), Inferior Frontal Gyrus (BA 47), Middle Frontal Gyrus (BA 10 and 11); Medial Frontal Gyrus (BA 10), Superior Frontal Gyrus (BA 6 and 10), Superior Temporal Gyrus (BA 22) and Middle Occipital Gyrus (BA 19) were the most frequent cortical activated areas for both **ID** and **PD**.

PCA showed that the amount of information $H(e_i)$, provided by each electrode e_i about the s_i involved in dilemma analysis, covaried according to 3 different patterns (P_1 , P_2 and P_3) that differed for **ID** and **PD** (PCA mappings in **Figure 4**). These patterns explained more than 80% of data covariance and have eigenvalues that ranged from 10 (P_1) to 1.12 (P_3).

Pattern P_1 was characterized by the electrodes O1, O2, OZ, P3, P4, PZ, T3, T4, T5 and T6, all of them having loadings greater than 0.6 in P_1 (**Table 1**) in **ID** case, and characterized by the electrodes O1, O2, OZ, P3, P4, PZ, T3 and T4 in **PD** case (PCA mappings in **Figure 4**). Therefore, the main P_1 difference when both types of dilemma are considered is the enrollment of T5 and T6 in **ID** analysis but not in **PD** analysis. Pattern P_2 , in contrast, was characterized by the same set of electrodes F4, F7, F8, FP1, FP2 and FZ for both **ID** and **PD**. Finally, pattern P_3 was characterized by the electrodes C3, C4, CZ and P4 in **ID** case, and by the electrodes T5 and T6 in **PD**.

Because the electrical activity recorded by each electrode is determined by the weighted summation of the electrical currents generated by each s_i , we identified those s_i at the nearest location l_i to the electrodes composing each PCA mapping P_1 , P_2 and P_3 . **Figure 4** shows also the spatial relation between the identified s_i and PCA mappings as well as their cortical locations and frequencies. Pattern P_1 is spatially associated with sources located at BAs 7, 18, 19, 20, 21 and 22 for both **ID** and **PD**, although the frequency s_i were located at these areas differed for each type of dilemma. Pattern P_2 is spatially associated with sources located at BAs 6, 8, 9, 10, 11, 42, 43, 44, 45, 46 and 47 in case of both **ID** and **PD** but location frequency also differed for both types of dilemma. Finally, pattern P_3 is spatially associated with sources located at BAs 1, 3, 4, 5, 6 and 7 in **ID** case and only at BA 21 in **PD** case;

The next step of our study focused on each (**D**, **A** and **J**) of phases of dilemma analysis without discriminating between **ID** and **PD**. **Figure 1** summarizes the results of this study showing the PCA mappings calculated from data in **Table 2** and the spatial location of the **ILS**.

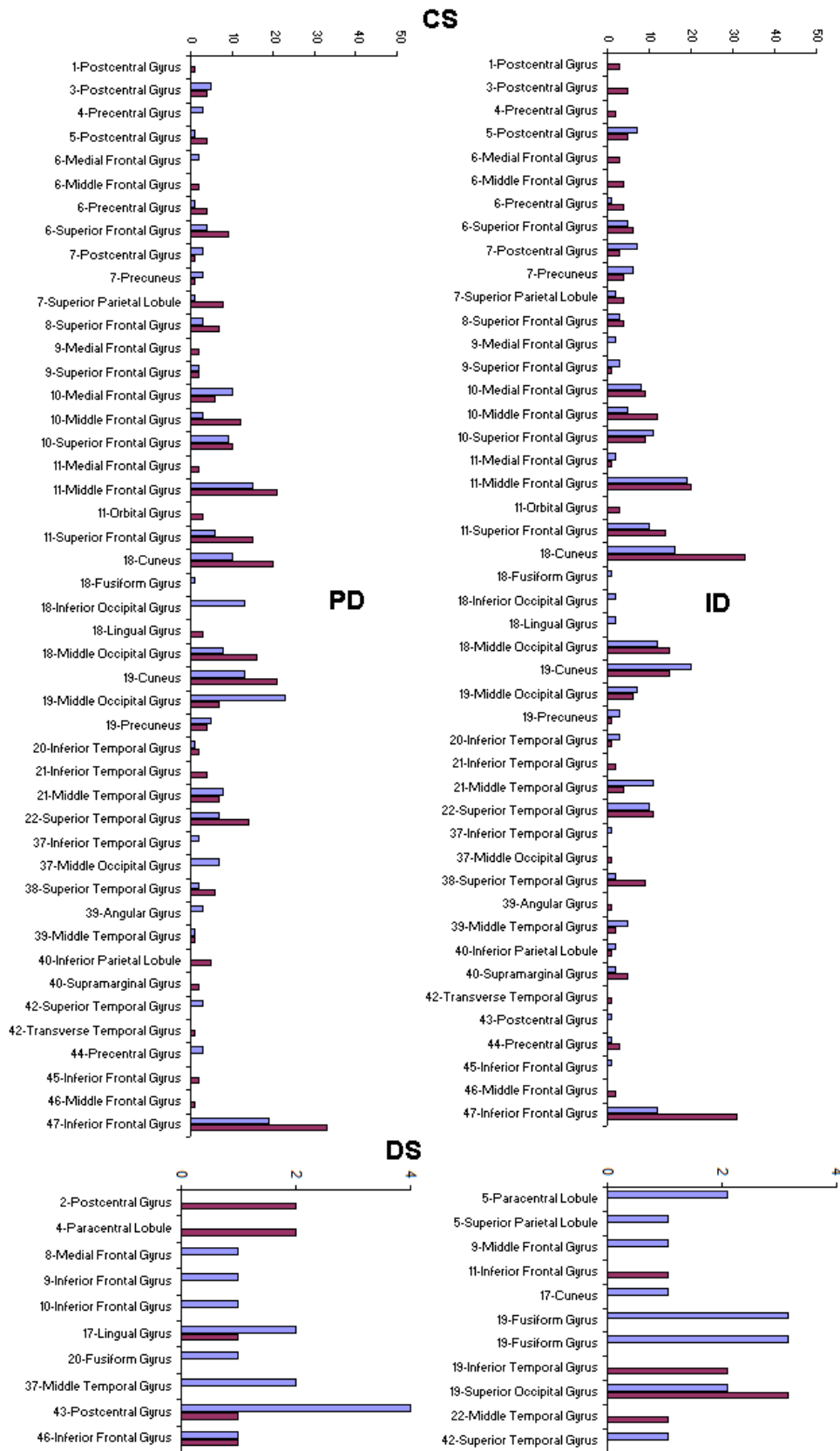


Figure 2. Identified Loreta Sources for PD and ID. CS—sources that are common to both dilemma types and DS—sources that uniquely identify either PD or ID.

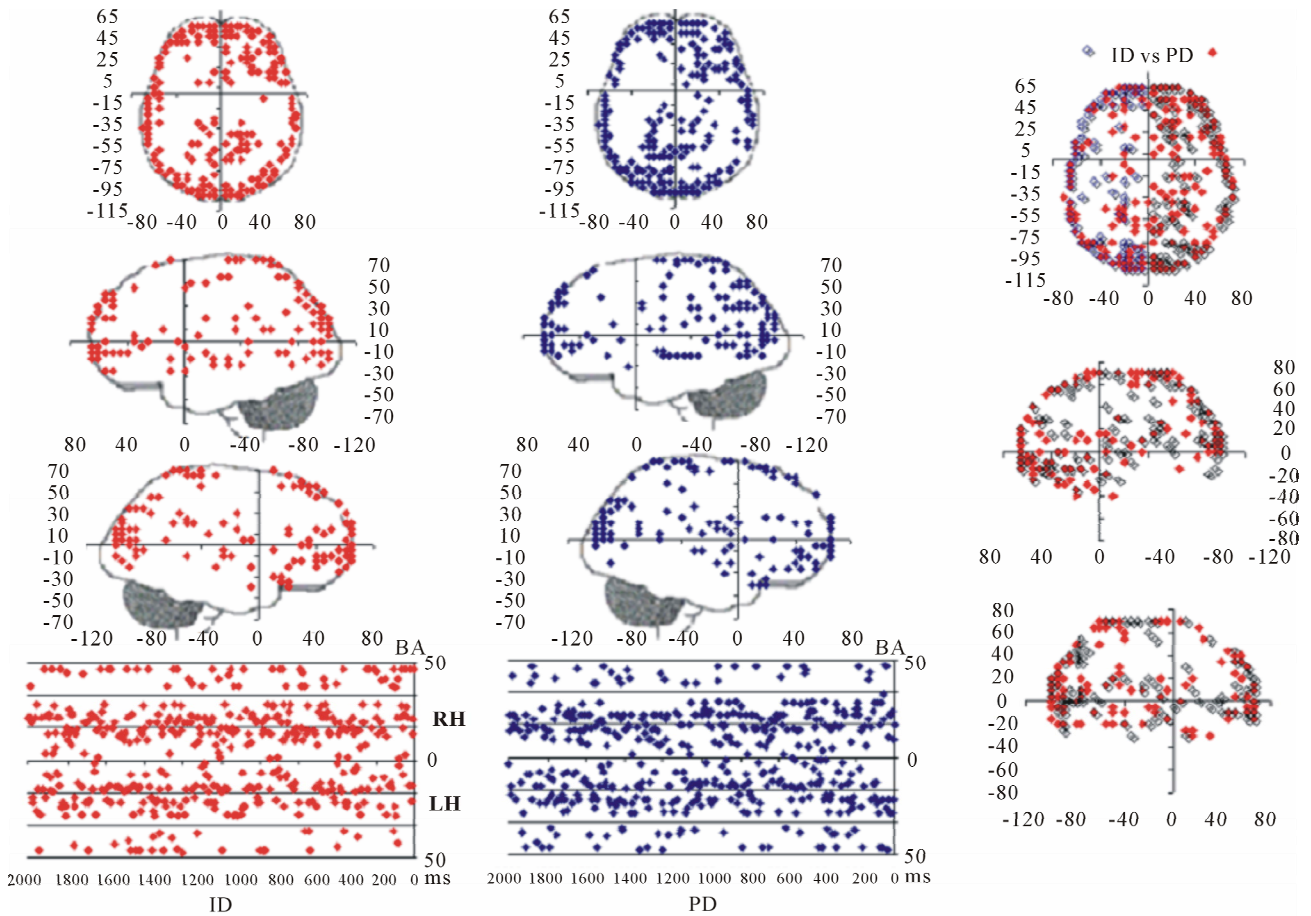


Figure 3. Spatial and temporal distribution of the identified Loreta sources for PD and ID. BA—Brodmann area number 4TH.

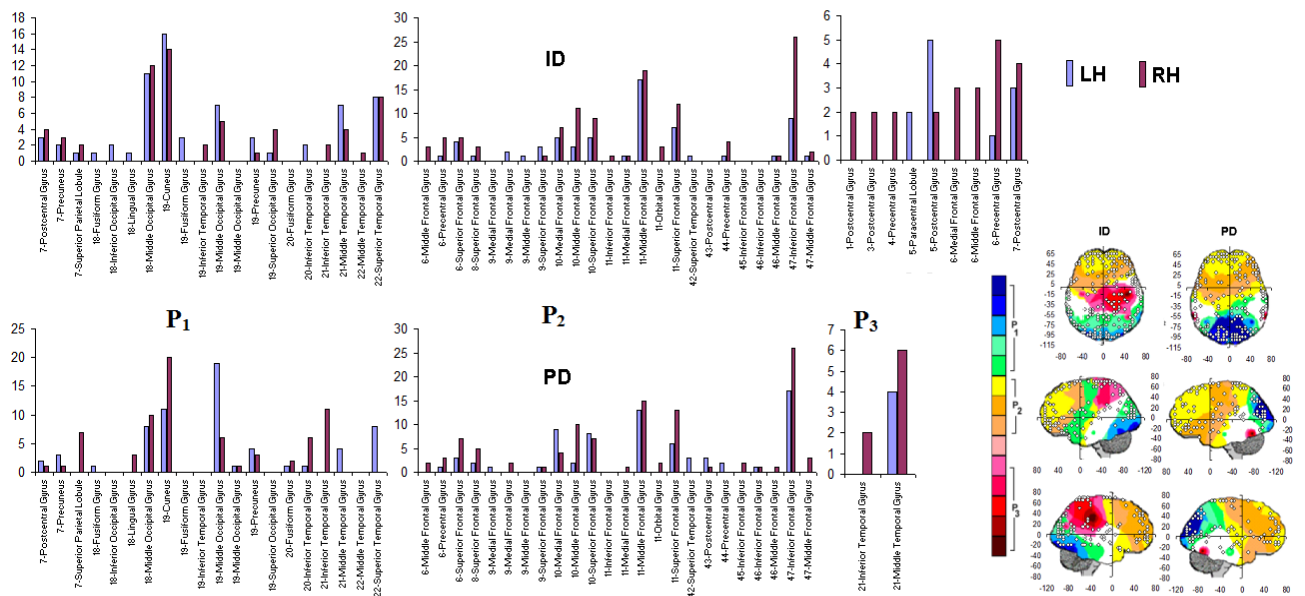


Figure 4. Identified Loreta sources and PCA mappings for ID and PD and comparison of source location for ID vs PD. PCA analysis revealed the existence of 3 patterns (P_1 , P_2 and P_3) of $H(e_i)$ covariation. PCA mappings were built with those factor loadings greater than 0.6 (bold) in Table 1. P_1 is colored green to blue, P_2 is colored yellow to brown and P_3 is colored rose to dark red. Cortical areas are defined by their BA number and anatomical location.

Table 1. $H(e_i)$ PCA results for ID and PD.

	ID			PD		
	P1	P2	P3	P1	P2	P3
C3	0.11	0.54	0.64	0.65	0.15	0.32
C4	0.30	0.17	0.82	0.39	0.21	0.61
CZ	0.31	0.40	0.61	0.54	0.21	0.40
F3	0.25	0.80	0.28	0.81	0.02	0.30
F4	0.15	0.59	0.40	0.69	0.16	0.25
F7	0.48	0.62	0.20	0.65	0.13	0.42
F8	0.49	0.47	0.24	0.54	0.18	0.49
FP1	0.36	0.81	0.11	0.80	-0.02	0.32
FP2	0.15	0.85	0.13	0.83	-0.03	0.19
FZ	0.22	0.85	0.12	0.85	-0.01	0.25
O1	0.83	0.28	0.16	0.33	0.02	0.78
O2	0.80	0.33	0.24	0.31	-0.02	0.82
OZ	0.74	0.30	0.24	0.32	0.01	0.73
P3	0.55	0.29	0.56	0.24	0.17	0.79
P4	0.57	0.08	0.66	0.22	0.02	0.84
PZ	0.60	0.15	0.53	0.18	0.06	0.81
T3	0.63	0.34	0.30	0.37	0.22	0.66
T4	0.64	0.13	0.45	0.29	0.32	0.68
T5	0.78	0.17	0.22	0.01	0.97	0.08
T6	0.81	0.29	0.25	0.03	0.97	0.05
Expl.Var	5.88	4.81	3.39	5.46	2.24	6.09
Prp.Totl	0.29	0.24	0.17	0.27	0.11	0.30

Table 2. $H(e_i)$ PCA results for the experimental steps D, A and J.

	D		A		J		
	P1	P2	P1	P2	P1	P2	P3
C3	0.40	0.66	0.45	0.60	0.26	0.42	0.64
C4	0.69	0.36	0.69	0.34	0.30	0.18	0.79
CZ	0.42	0.57	0.51	0.57	0.19	0.34	0.72
F3	0.32	0.80	0.30	0.84	0.29	0.78	0.24
F4	0.32	0.64	0.25	0.75	-0.02	0.68	0.41
F7	0.48	0.65	0.55	0.60	0.49	0.46	0.43
F8	0.51	0.58	0.57	0.52	0.45	0.44	0.38
FP1	0.37	0.79	0.41	0.77	0.45	0.72	0.23
FP2	0.12	0.87	0.17	0.87	0.19	0.87	0.05
FZ	0.21	0.88	0.21	0.85	0.33	0.82	0.18
O1	0.83	0.31	0.82	0.33	0.82	0.24	0.25
O2	0.86	0.30	0.85	0.31	0.83	0.28	0.27
OZ	0.75	0.30	0.79	0.32	0.75	0.30	0.25
P3	0.73	0.34	0.79	0.31	0.53	0.19	0.68
P4	0.83	0.19	0.81	0.24	0.49	0.13	0.71
PZ	0.80	0.23	0.82	0.19	0.59	0.15	0.54
T3	0.65	0.41	0.67	0.41	0.47	0.32	0.51
T4	0.77	0.27	0.77	0.26	0.51	0.16	0.56
T5	0.82	0.22	0.80	0.22	0.78	0.22	0.26
T6	0.84	0.29	0.84	0.31	0.81	0.26	0.28
Expl.Var	7.95	5.71	8.32	5.63	5.61	4.30	4.40
Prp.Totl	0.40	0.29	0.42	0.28	0.28	0.22	0.22

A total of 469 possible sources s_i of the averaged EEG for **D**, **A** and **J** phases were identified in 47 (**A**) to 62 (**J**) different cortical locations (l_i) because their calculated Z score was greater than 2. Of these locations, 6 sets of ranging from 7 to 15 locations that were identified as unique and distinctive sources (DS) for each phase.

PCA showed that the amount of information $H(e_i)$ provided by each electrode l_i about the s_i covaried according to 2 different patterns P₁ and P₂ during both **D** and **A** phases and according to 3 patterns P₁, P₂ and P₃ in case of **J**, having eigenvalues ranging from 9.83 to 1.23 and explaining around 70% of data covariance. Pattern P₁ was characterized by the electrodes (loadings greater than 0.6) O1, O2, OZ, P3, P4, PZ, T3, T4, T5 and T6 for both **D** and **A** phases. In similar way, Pattern P₁ was characterized by the electrodes F4, F7, FP1, FP2 and FZ for both **D** and **A** phases. Finally, pattern P₃ that occurred only during **J**, was characterized by the electrodes C3, C4, CZ, P3 and P4.

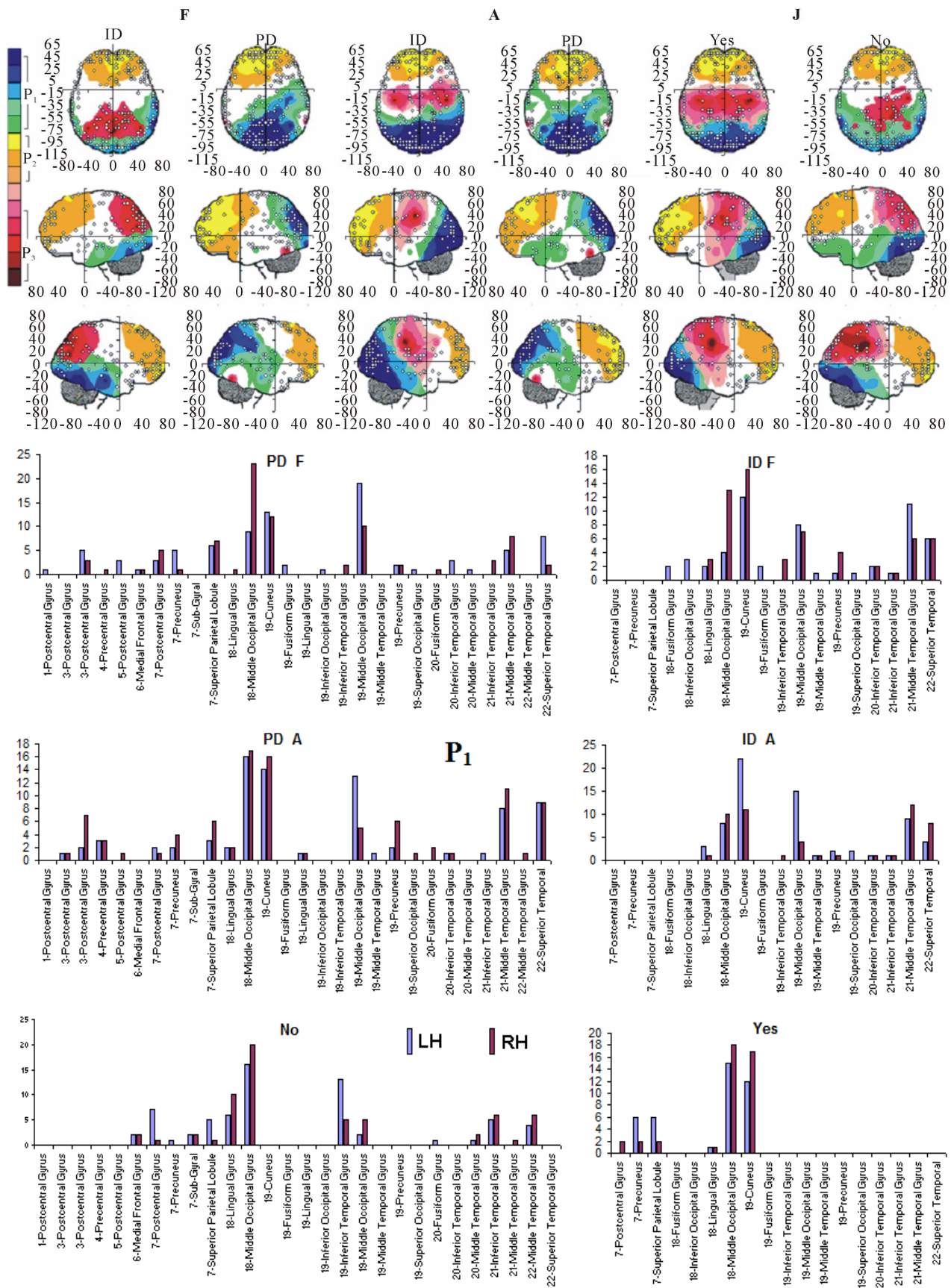
Pattern P₁ is spatially associated in case **F** and **A** phases, with sources located at anterior BAs 1 to 7, at posterior BAs 17 to 19, at temporal BAs 20 to 22 and BAs 37 to 39, at parietal BA 40, besides at insula and cingulated gyrus. In case of **D** phase, pattern P₁ is spatially associated with a different set of sources that excluded, in comparison to phases **F** and **A**, the BAs 1 to 6, some of the locations at BAs 18 and 19, while including the parahippocampal gyrus. Pattern P₂ is spatially associated with sources located at BAs 6 to 11 for all experimental phases. Finally, in case of **D** phase, pattern P₃ is spatially associated with sources located at anterior BAs 1 to 7, that were excluded from the set of sources associated with pattern P₁ in case **F** and **A** phases.

The final step of our analysis focused on each of **D**, **A** and **J** phases of dilemma discriminated by dilemma type (**D** and **A**) and judgment type. A total that ranged from 328 to 453 possible sources s_i of the averaged EEG for **D**, **A** and **J** phases were identified in 53 to 61 different cortical locations (l_i) because their calculated Z score was greater than 2. 3 to 10 of these locations were identified as unique and distinctive sources (DS) for each phase and each dilemma type or judgment.

PCA showed that the amount of information $H(e_i)$ provided by each electrode e_i about the e_i covaried, for all studied conditions, according to 3 patterns (P₁, P₂ and P₃) that have eigenvalues ranging from 9.76 to 1.11 and explained around 70% of data covariance (**Figure 5** and **Table 3**). In **ID** case, pattern P₁ included electrodes O1, O2, OZ, T3, T4, T5 and T6 for both phases **F** and **A**, and included electrodes P3, P4 and PZ in **F** case. Pattern P₂ included electrodes F3, FP1, FP2 and FZ for both phases **F** and **A**. Finally, pattern P₃ included electrodes C4, P3, P4 and PZ in **F** case and C3, C4 and CZ in **F** case. In **PD** case, pattern P₁ included electrodes O1, O2, OZ,

Table 3. $H(e_i)$ PCA results for the experimental steps D, A and J.

	ID			F	PD				ID			A	PD		
	P1	P2	P3		P1	P2	P3		P1	P2	P3		P1	P2	P3
C3	0.24	0.66	0.43	0.09	0.57	0.66	C3	0.28	0.68	0.05	0.32	0.63	0.28		
C4	0.33	0.21	0.84	0.42	0.13	0.76	C4	0.67	0.37	0.05	0.54	0.44	0.29		
CZ	0.28	0.51	0.65	0.41	0.31	0.65	CZ	0.36	0.51	0.13	0.35	0.62	0.31		
F3	0.25	0.79	0.27	0.28	0.82	0.28	F3	0.35	0.77	0.06	0.33	0.82	-0.02		
F4	0.07	0.61	0.48	0.26	0.53	0.52	F4	0.42	0.55	0.17	0.16	0.77	0.13		
F7	0.54	0.70	0.00	0.46	0.65	0.17	F7	0.37	0.70	0.11	0.49	0.61	0.05		
F8	0.46	0.63	0.11	0.50	0.44	0.32	F8	0.52	0.53	0.04	0.51	0.55	0.25		
FP1	0.33	0.81	0.09	0.36	0.86	0.08	FP1	0.30	0.82	-0.08	0.37	0.77	-0.02		
FP2	0.08	0.87	0.15	0.21	0.86	0.16	FP2	0.20	0.83	0.01	0.21	0.83	-0.13		
FZ	0.20	0.88	0.13	0.14	0.84	0.16	FZ	0.22	0.86	0.03	0.24	0.85	0.00		
O1	0.88	0.26	0.08	0.80	0.33	0.14	O1	0.81	0.38	-0.02	0.79	0.34	0.01		
O2	0.80	0.25	0.34	0.79	0.38	0.19	O2	0.82	0.34	-0.02	0.86	0.28	0.03		
OZ	0.76	0.20	0.31	0.72	0.39	0.18	OZ	0.65	0.37	-0.01	0.81	0.25	0.10		
P3	0.64	0.36	0.36	0.71	0.29	0.35	P3	0.75	0.26	0.08	0.82	0.23	0.21		
P4	0.61	0.08	0.65	0.77	0.13	0.30	P4	0.86	0.18	-0.02	0.84	0.26	-0.04		
PZ	0.67	0.15	0.49	0.74	0.20	0.20	PZ	0.79	0.19	0.15	0.84	0.17	0.02		
T3	0.68	0.48	0.08	0.64	0.34	0.33	T3	0.68	0.31	0.20	0.67	0.37	0.21		
T4	0.61	0.26	0.46	0.69	0.09	0.48	T4	0.75	0.23	0.27	0.64	0.28	0.45		
T5	0.75	0.20	0.24	0.79	0.18	0.12	T5	0.08	0.01	0.98	0.08	0.00	0.95		
T6	0.76	0.23	0.39	0.78	0.37	0.22	T6	0.03	0.02	0.98	0.04	0.00	0.96		
Expl.Var	6.17	5.52	3.01	6.69	5.00	2.72	Expl.Var	6.27	5.33	2.14	6.37	5.53	2.47		
Prp.Totl	0.31	0.28	0.15	0.33	0.25	0.14	Prp.Totl	0.31	0.27	0.11	0.32	0.28	0.12		
					Yes				No						
					P1	P2	P3		P1	P2	P3				
				C3	0.10	0.54	0.71		0.34	0.54	0.52				
				C4	0.40	0.32	0.75		0.27	0.34	0.77				
				CZ	0.29	0.41	0.65		0.27	0.46	0.67				
				F3	0.18	0.81	0.37		0.37	0.79	0.17				
				F4	0.06	0.76	0.41		-0.05	0.72	0.52				
				F7	0.52	0.64	0.29		0.55	0.46	0.40				
				F8	0.67	0.47	0.21		0.40	0.54	0.48				
				FP1	0.33	0.83	0.18		0.52	0.63	0.34				
				FP2	0.15	0.87	0.16		0.33	0.84	0.10				
				FZ	0.39	0.84	0.08		0.35	0.79	0.20				
				O1	0.86	0.22	0.13		0.74	0.22	0.46				
				O2	0.90	0.25	0.13		0.83	0.28	0.34				
				OZ	0.83	0.23	0.15		0.71	0.30	0.36				
				P3	0.61	0.19	0.56		0.51	0.24	0.69				
				P4	0.67	0.12	0.58		0.47	0.12	0.74				
				PZ	0.72	0.16	0.42		0.45	0.18	0.69				
				T3	0.49	0.24	0.57		0.54	0.42	0.48				
				T4	0.39	0.46	0.56		0.69	0.34	0.20				
				T5	0.75	0.21	0.42		0.85	0.26	0.22				
				T6	0.82	0.24	0.26		0.86	0.28	0.23				
				Expl.Var	6.50	5.20	3.77		6.00	4.76	4.36				
				Prp.Totl	0.3	0.26	0.2		0.3	0.2	0.22				



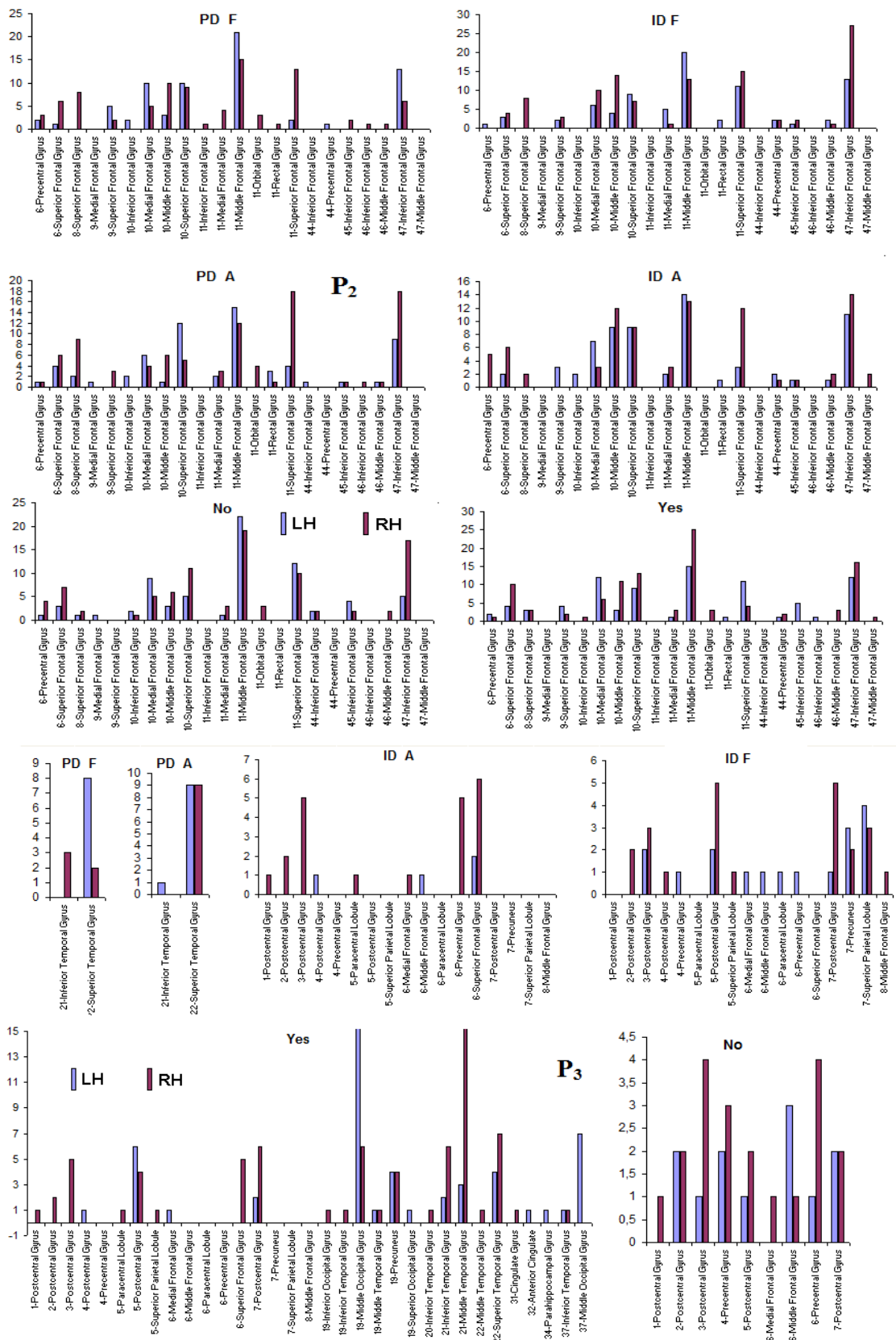


Figure 5. Identified Loretta sources and PCA mappings for ID and PD during F and A and for Yes and No judgments during J. PCA mappings were built with those factor loadings greater than 0.6 (bold) in Table 3.

P3, P4, PZ, T3 and T4; pattern P_2 included electrodes F3, F4, FP1, FP2 and FZ and pattern P_3 included electrodes T5 and T6. **Yes** and **NO** judgments were associated with a pattern P_1 that included electrodes O1, O2, OZ, P3, P4, PZ, T5 and T6; pattern P_2 that included electrodes F3, FP1, FP2 and FZ, pattern P_3 that included C4, CZ, P3, P4 and PZ. C3 electrode was also included in P_3 in case of **Yes** judgment.

Pattern P_1 is spatially associated (**Figure 5**) with sources located at anterior BAs 1-7, posterior BAs 18-19 and temporal BAs 20 to 22, in cases of **PD F** and **PD A** phases as well as **No** decisions. However, differences on S_i location frequencies at these cortical areas were observed between mostly between **No** decisions and **PD** phases. In addition, in cases of **ID F** and **ID A** phases, pattern P_1 is spatially associated with sources located at anterior BA 7, posterior BAs 18 and 19, and temporal BAs 20 to 22. Finally, in case of **Yes** decisions, pattern P_1 is spatially associated with sources located at anterior BA7 and BAs 18 and 19. Summing up, PCA pattern P_1 is associated with very different set of sources if **PD** and **ID** or **Yes** and **No** responses are compared. Pattern P_2 is spatially associated with sources located at BAs 6 to 11 and 44 to 47 for all phases, dilemma type and judgment response, being therefore determined almost by the same sources with slightly location frequencies at these areas. Finally, pattern P_3 is the most variable according to their generation sources, being associated only with Inferior (ITG) and Superior Temporal (STG) cortices in case of **PD F** and **PD A** phases; with sources located at BAs 1 to 8 in case of **ID F** and **ID A** phases; BAs 1 to 7 for **No** responses; and located at BAs 1 to 8, BAs 118 to 19, BAs 20 to 22 besides ITG, STG and cingulated cortices.

Logistic regression analysis showed that dilemma judgment J correlates with $H(e_i)$ and explains for around 70% of the decisions and that gender is influential on these correlations at the statistical level of $p = 0.005$. Although there are some differences between regression mappings **D**, **A** and **J** in **Figure 6**, it may be said that high $H(e_i)$ at middle line electrodes (light green to dark blue) favor $J = \text{Yes}$ while left and occipital electrodes (rose to dark red) favor $J = \text{No}$. **Table 1** correlates the regression mappings **D**, **A** and **J** and their corresponding ILS. It is interesting to note that differential intercept coefficients in **G** and the angular coefficients in **D**, **A** and **J** tended to be of opposite signals. Middle line electrodes in **G** are negative and in the other mappings they are positive. This means that woman would decide for a **Yes** judgment with values of $H(e_i)$ smaller than those required in case of man for the same judgment. Differential intercept coefficients for electrodes FP2, C3, OZ and O2 were positive, while their corresponding angular coefficients are negative. This means that to decide for a **No** judgment, woman shall have values of $H(e_i)$

smaller than those required in case of man for the same judgment.

4. Discussion

As predicted, both the number of ILSs and the number of their instantiations during dilemma judgment were very high in comparison with the fMRI identified locations associated with either **ID** and/or **PD**. These results are consequence from the high EEG temporal resolution as compared to fMRI. ILS were identified a mean rate of 20ms while fMRI demands in general 2 seconds to detect reliable hemodynamic changes associated with the studied cognitive task. In addition, both **ISLs** and **PCA** patterns differed between **ID** and **PD**, as well as for **D**, **A** and **J** and **Yes/No** judgment. That (almost) all **ILSs** are also functionally related with dilemma judgment follows from the discussion below.

Moral dilemma judgment requires most of (if not all) times a decision about a hypothetical problem that was never experienced by the individual (e.g., foot bridge and trolley dilemma) or at most that has occurred but not was experienced by the other than throughout the media (e.g., Andes aircraft crash). This implies that dilemma solution demands simulations of the benefit of avoiding loss predicted by **F** and of the adequacy of action proposed by **A** to avoid social loss taking into consideration personal risk in implementing it [1]. If adequacy is high then willingness to implement action (**Yes** judgment) is also high, otherwise the willingness to not implement action (**No** judgment) will predominate.

Benefit and risk simulations are supposed to take profit of individual knowledge and their autobiographic history [17-20]. Therefore they required involvement of working memory that are supposed to be supported by the activity of neurons in many cortical sites, as Dorsolateral Frontal Cortex, Precuneus, Cuneus and others [21-28]. In addition, risk and benefit evaluations were proved to be dependent on participation of neurons distributed over various cortical areas, as Orbitofrontal cortex [29-33]; Medial Prefrontal cortex [34]; insula [35], among others. Adequacy and willingness to act, in turn, involve participation of many parietal sites [36-38] and competition between alternative actions, mostly those personal and social alternatives, is handled by Inferior Frontal Cortex [39-41]. Therefore, it is expected that dilemma analysis and judgment demands the enrollment of neurons widely distributed of many different cortical sites, as observed in the present paper.

Let be proposed that **PCA** pattern P_1 characterizes those electrodes providing information about **ILSs** involved in carrying out the above required simulations. This proposition derives from the fact that sources associated with P_1 are mostly located in Inferior Frontal Cortex, Temporoparietal junction, Superior Temporal Sulcus,

Cuneus and Precuneus, all of them reported as associated with mentalizing, memory and autobiographic memory (e.g., [19,20,42-45]). In addition, we may assume that P_2 characterizes those electrodes providing information about **ILSs** involved in both benefit and risk assessment as well using these data to control simulations and the calculus of action adequacy and willingness to act. This proposition derives from the fact that sources associated with P_2 are mostly located at Medial Frontal Cortex, Dorsolateral Frontal Cortex, Orbitofrontal Cortex, Inferior Frontal Cortex, Superior Frontal Cortex, all of them reported as associated with risk and benefit assessment, attention control, working memory control, etc. [8,9,18,19,22,29,31,40,41,43]. Finally, it may be also considered that PCA pattern P_3 characterizes those electrodes providing information about **ILSs** involved in carrying out the calculations of action adequacy and willingness to act, because associated with P_2 are mostly located at SII, Paracentral Gyrus, Inferior and Superior Parietal Lobule and Temporal Pole. These areas have been reported as associated with planning and intention (e.g., [36-38]).

Now, if it is accepted that personal risk is high in **PD** case in comparison to **ID**, then PCA mappings differences observed here, concerning dilemma type and judgment phase may be understood taking into consid-

eration that as risk increases in relation to benefit, conflict in decision making also increases [1], requiring harder simulations to reach a final dilemma judgment. This implies that **PD** judgment is experienced as harder than decision in **ID** case, demanding more simulations and therefore being associated with a more persistent and larger P_2 , as well as postponing the organization of P_3 that may occur only in **J** phase. In this context, cognition and emotion play complementary instead of opposing roles in dilemma judgment as proposed by [3].

These conclusions are supported by the results of logistic regression analysis that showed that dilemma judgment J is a linear function of $H(e_i)$ showing a) that middle line and left frontal (in **A** and **J**) electrodes and left frontal provides information about sources located at BA 4, 7, 9, 10, 11, 18, 19 and 42 (**Table 4**) that are influential on supporting action proposed in **A** ($J = Yes$) as dilemma solution, and b) electrodes located mostly at the left hemisphere providing information about sources at BA 4, 5, 6, 7, 9, 10, 11 and 47 that are influential in not supporting action proposed in **A** ($J = No$) as dilemma solution. This result greatly expands our knowledge about how intended moral value is calculated by brain beyond that provided by [4]. In addition, our results also clearly points for gender differences in dilemma judgment that are influential over the above cir-

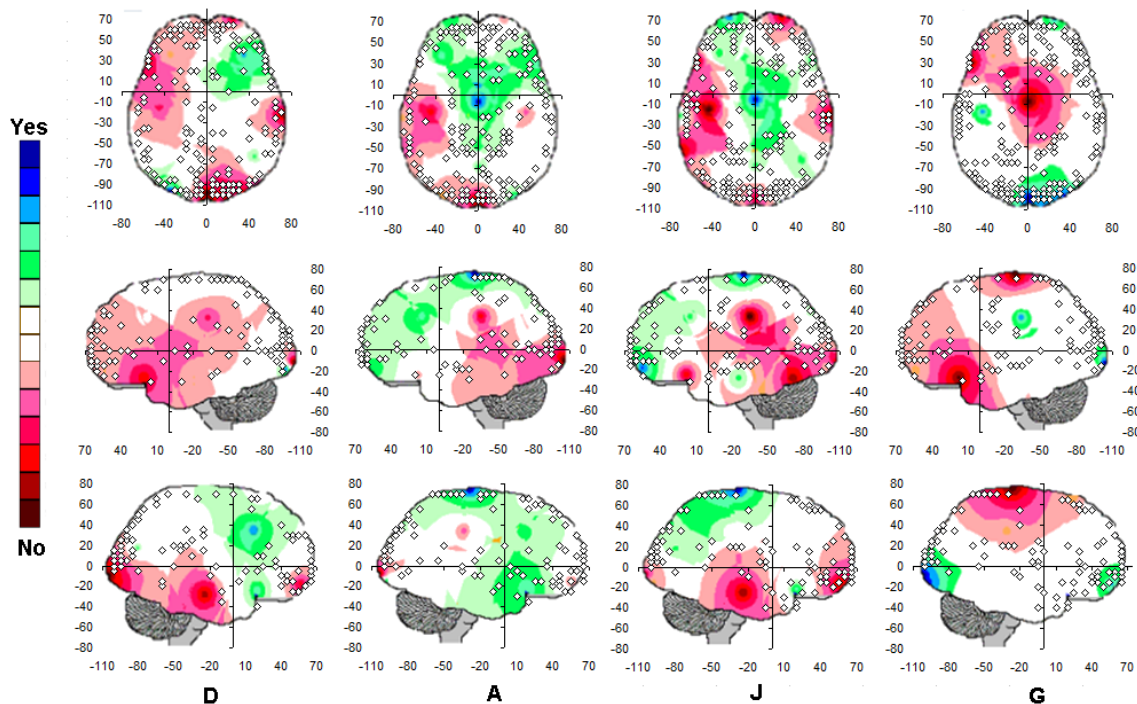


Figure 6. Logistic Regression Mappings showing the correlation between Yes/No decision and $H(e_i)$ calculated for analysis phases D, A and J, and gender influence (G) on these regressions. The spatial locations of Loreta Sources for corresponding phases are superposed. Negative angular coefficients (β_i) are encoded in rose to dark red and positive angular coefficients are encoded from light green to dark blue. Statistically non significant β_i are white encoded.

Table 4. Loreta sources associated with regression mappings D, A, J and G.

D	A	J	G
Positive Beta	Positive Beta	Positive Beta	Positive Beta
6-Superior Frontal Gyrus	4-Precentral Gyrus	4-Precentral Gyrus	4-Precentral Gyrus
10-Superior Frontal Gyrus	5-Paracentral Lobule	5-Postcentral Gyrus	7-Superior Parietal Lobule
11-Middle Frontal Gyrus	5-Postcentral Gyrus	6-Middle Frontal Gyrus	9-Superior Frontal Gyrus
18-Posterior Cingulate	6-Medial Frontal Gyrus	6-Precentral Gyrus	10-Inferior Frontal Gyrus
18-Inferior Occipital Gyrus	6-Middle Frontal Gyrus	6-Superior Frontal Gyrus	10-Medial Frontal Gyrus
18-Fusiform Gyrus	6-Precentral Gyrus	7-Postcentral Gyrus	10-Middle Frontal Gyrus
18-Middle Occipital Gyrus	6-Superior Frontal Gyrus	7-Precuneus	10-Superior Frontal Gyrus
17-Lingual Gyrus	7-Cuneus	10-Middle Frontal Gyrus	11-Inferior Frontal Gyrus
18-Cuneus	7-Postcentral Gyrus	10-Superior Frontal Gyrus	11-Medial Frontal Gyrus
18-Posterior Cingulate	7-Precuneus	11-Inferior Frontal Gyrus	18-Fusiform Gyrus
18-Inferior Occipital Gyrus	7-Superior Parietal Lobule	11-Medial Frontal Gyrus	18-Lingual Gyrus
18-Fusiform Gyrus	9-Superior Frontal Gyrus	11-Middle Frontal Gyrus	18-Middle Occipital Gyrus
18-Lingual Gyrus	10-Inferior Frontal Gyrus	11-Rectal Gyrus	19-Cuneus
18-Middle Occipital Gyrus	10-Medial Frontal Gyrus	11-Superior Frontal Gyrus	19-Inferior Temporal Gyrus
19-Cuneus	10-Middle Frontal Gyrus	45-Inferior Frontal Gyrus	19-Lingual Gyrus
19-Inferior Temporal Gyrus	10-Superior Frontal Gyrus	46-Inferior Frontal Gyrus	19-Middle Occipital Gyrus
19-Middle Occipital Gyrus	11-Inferior Frontal Gyrus	46-Middle Frontal Gyrus	19-Middle Temporal Gyrus
19-Precuneus	11-Medial Frontal Gyrus	47-Inferior Frontal Gyrus	19-Precuneus
44-Precentral Gyrus	10-Middle Frontal Gyrus	47-Inferior Frontal Gyrus	19-Inferior Occipital Gyrus
45-Inferior Frontal Gyrus	10-Superior Frontal Gyrus		42-Superior Temporal Gyrus
46-Middle Frontal Gyrus	11-Inferior Frontal Gyrus	Negative Beta	
47-Inferior Frontal Gyrus	11-Medial Frontal Gyrus	18-Fusiform Gyrus	Negative Beta
	11-Middle Frontal Gyrus	18-Lingual Gyrus	4-Precentral Gyrus
Negative Beta	11-Orbital Gyrus	18-Middle Occipital Gyrus	5-Postcentral Gyrus
9-Superior Frontal Gyrus	11-Rectal Gyrus	19-Cuneus	6-Middle Frontal Gyrus
10-Inferior Frontal Gyrus	11-Superior Frontal Gyrus	19-Inferior Temporal Gyrus	6-Precentral Gyrus
10-Medial Frontal Gyrus	44-Precentral Gyrus	19-Middle Occipital Gyrus	6-Superior Frontal Gyrus
10-Middle Frontal Gyrus	45-Inferior Frontal Gyrus	19-Middle Temporal Gyrus	7-Postcentral Gyrus
10-Superior Frontal Gyrus	46-Middle Frontal Gyrus	19-Precuneus	7-Superior Parietal Lobule
11-Inferior Frontal Gyrus	47-Inferior Frontal Gyrus	20-Inferior Temporal Gyrus	9-Superior Frontal Gyrus
11-Medial Frontal Gyrus		21-Inferior Temporal Gyrus	10-Inferior Frontal Gyrus
17-Lingual Gyrus	Negative Beta	21-Middle Temporal Gyrus	10-Medial Frontal Gyrus
18-Cuneus	18-Fusiform Gyrus	37-Middle Occipital Gyrus	10-Middle Frontal Gyrus
18-Posterior Cingulate	18-Lingual Gyrus	38-Superior Temporal Gyrus	10-Superior Frontal Gyrus
18-Inferior Occipital Gyrus	18-Middle Occipital Gyrus	39-Angular Gyrus	11-Inferior Frontal Gyrus
18-Fusiform Gyrus	19-Cuneus	39-Inferior Parietal Lobule	11-Medial Frontal Gyrus
18-Lingual Gyrus	19-Inferior Temporal Gyrus	39-Middle Temporal Gyrus	47-Inferior Frontal Gyrus
18-Middle Occipital Gyrus	19-Lingual Gyrus	39-Superior Temporal Gyrus	
19-Cuneus	19-Middle Occipital Gyrus	40-Inferior Parietal Lobule	
19-Inferior Temporal Gyrus	19-Middle Temporal Gyrus	40-Postcentral Gyrus	
19-Middle Occipital Gyrus	19-Precuneus	40-Supramarginal Gyrus	
19-Precuneus	19-Inferior Occipital Gyrus	42-Superior Temporal Gyrus	
19-Superior Occipital Gyrus	20-Inferior Temporal Gyrus	42-Transverse Temporal Gyrus	
20-Inferior Temporal Gyrus	20-Fusiform Gyrus	43-Postcentral Gyrus	
20-Fusiform Gyrus	21-Inferior Temporal Gyrus	45-Inferior Frontal Gyrus	
21-Middle Temporal Gyrus	21-Middle Temporal Gyrus	46-Inferior Frontal Gyrus	
22-Superior Temporal Gyrus	22-Middle Temporal Gyrus	46-Middle Frontal Gyrus	

Continued

22-Superior Temporal Gyrus
 23-Cuneus
 37-Fusiform Gyrus
 37-Inferior Temporal Gyrus
 37-Middle Temporal Gyrus
 37-Middle Occipital Gyrus
 38-Superior Temporal Gyrus
 39-Middle Temporal Gyrus
 39-Superior Temporal Gyrus
 40-Inferior Parietal Lobule

47-Inferior Frontal Gyrus

circuits supporting Yes and No judgments.

5. Conclusions

Summing up we may conclude that present results clearly support initial hypotheses that:

- 1) $H(e_i)$ PCA analysis will identify the most important patterns of temporal and spatial correlation between these ILSs associated with dilemma analysis, and
- 2) dilemma judgment has to be the result of the enrollment of many different neural circuits in charge to evaluate benefits and risks associated with **D** and **A** and using these evaluations to calculate the adequacy of action proposed in **A** as its solution, as well as the willingness of implementing or not the proposed solution.

REFERENCES

- [1] A. F. Rocha, M. N. Burattini, F. T. Rocha and E. Massad, "A Neuroeconomic Modeling of Attention-deficit/Hyperactivity Disorder (ADHD)," *Journal of Biological Systems*, Vol. 17, 2009, pp. 597-622.
<http://dx.doi.org/10.1142/S021833900900306X>
- [2] J. D. Greene, R. B. Sommerville, L. E. Nystrom, J. M. Darley and J. D. Cohen, "An fMRI Investigation of Emotional Engagement in Moral Judgment," *Science*, Vol. 293, No. 5537, 2001, pp. 2105-2108.
<http://dx.doi.org/10.1126/science.1062872>
- [3] J. D. Greene, L. E. Nystrom, A. D. Nystrom, A. D. Engel, J. M. Darley and J. D. Cohen, "The Neural Bases of Cognitive Conflict and Control in Moral Judgment," *Neuron*, Vol. 44, No. 2, 2004, pp. 389-400.
<http://dx.doi.org/10.1016/j.neuron.2004.09.027>
- [4] A. Shenhav and J. D. Greene, "Moral Judgments Recruit Domain-General Valuation Mechanisms to Integrate Representations of Probability and Magnitude," *Neuron*, Vol. 67, No. 4, 2010, pp. 667-677.
<http://dx.doi.org/10.1016/j.neuron.2010.07.020>
- [5] J. Bentham, "The Principles of Morals and Legislation (Great Books in Philosophy)," 1988 Edition, New York. Prometheus Books.
- [6] R. D. Pascual-Marqui, "Standardized Low Resolution Brain Electromagnetic-Tomography (sLORETA): Technical Details," *Methods and Findings in Experimental and Clinical Pharmacology*, Vol. 24, 2002, pp. 5-12.
- [7] R. Adorni and A. M. Proverbio, "The Neural Manifestation of the Word Concreteness Effect: An Electrical Neuroimaging Study," *Neuropsychologia*, Vol. 50, No. 5, 2012, pp. 880-891.
<http://dx.doi.org/10.1016/j.neuropsychologia.2012.01.028>
- [8] M. Esslen, R. D. Pascual-Marqui, D. Hell, K. Kochi and D. Lehmann, "Brain Areas and Time Course of Emotional Processing," *NeuroImage*, Vol. 21, No. 4, 2004, pp. 189-1203.
<http://dx.doi.org/10.1016/j.neuroimage.2003.10.001>
- [9] J. J. Foxe and A. C. Snyder, "The Role of Alpha-Band Brain Oscillations as a Sensory Suppression Mechanism during Selective Attention," *Frontiers in Psychology*, Vol. 2, 2011, pp. 1-13
<http://dx.doi.org/10.3389/fpsyg.2011.00154>
- [10] C. M. Gómez, J. Marco-Pallarés and C. Graub, "Location of Brain Rhythms and Their Modulation by Preparatory Attention Estimated by Current Density," *Brain Research*, Vol. 1107, No. 1, 2006, pp. 151-160.
<http://dx.doi.org/10.1016/j.brainres.2006.06.019>
- [11] Y. Jiang, J. Lianekhammy, A. Lawson, C. Guo, D. Lyman, J. E. Joseph, B. T. Gold and T. H. Kelly, "Brain Responses to Repeated Visual Experience among Low and High Sensation Seekers: Role of Boredom Susceptibility Psychiatry Research," *Neuroimaging*, Vol. 173, 2009, pp. 100-106
- [12] T. K. G. Maeno, K. Iramina, F. Eto and S. Ueno, "Event-Related Potential P2 Derived from Visual Attention to the Hemi-Space. Source Localization with Loreta," *International Congress Series*, Vol. 1270, 2004, pp. 262-265.
<http://dx.doi.org/10.1016/j.ics.2004.04.034>
- [13] F. T. Rocha, A. F. Rocha, E. Massad and R. X. Menezes, "Brain Mappings of the Arithmetic Processing in Children and Adults," *Cognitive Brain Research*, Vol. 22, No. 3, 2005, pp. 359-372.
<http://dx.doi.org/10.1016/j.cogbrainres.2004.09.008>
- [14] A. F. Rocha, F. T. Rocha, M. N. Burattini and E. Massad, "Neurodynamics of an Election," *Brain Research*, Vol. 1351, 2010, pp. 198-211.
<http://dx.doi.org/10.1016/j.brainres.2010.06.046>
- [15] A. F. Rocha, F. T. Rocha and E. Massad, "The Brain as a Distributed Intelligent Processing System: An EEG Study," *PLoS One*, Vol. 6, No. 3, 2011, Article ID: E17355.
<http://dx.doi.org/10.1371/journal.pone.0017355>

- [16] C. L. Harenski and S. Hamann, "Neural Correlates of Regulating Negative Emotions Related to Moral Violations," *Neuroimage*, Vol. 30, No. 1, 2006, pp. 313-324. <http://dx.doi.org/10.1016/j.neuroimage.2005.09.034>
- [17] S. W. Chang, J.-F. Gariépy and M. L. Platt, "Neuronal Reference Frames for Social Decisions in Primate Frontal Cortex," *Nature Neuroscience*, Vol. 16, 2010, pp. 243-250. <http://dx.doi.org/10.1038/nn.3287>
- [18] A. Ikkai and C. E. Curti, "Common Neural Mechanisms Supporting Spatial Working Memory, Attention and Motor Intention," *Neuropsychologia*, Vol. 49, No. 6, 2011, pp. 1428-1434. <http://dx.doi.org/10.1016/j.neuropsychologia.2010.12.020>
- [19] R. L. E. P. Reniers, R. Corcoran, B. A. Völlm, A. Mashru, R. Howard and P. F. Liddle, "Moral Decision-Making, ToM, Empathy and the Default Mode Network," *Biological Psychology*, Vol. 90, No. 3, 2012, pp. 202-210. <http://dx.doi.org/10.1016/j.biopsycho.2012.03.009>
- [20] L. van der Meer, N. A. Groenewold, W. A. Nolen, M. Pijnenborg and A. Alema, "Inhibit Yourself and Understand the Other: Neural Basis of Distinct Processes Underlying Theory of Mind," *Neuroimage*, Vol. 56, No. 4, 2011, pp. 2364-2374. <http://dx.doi.org/10.1016/j.neuroimage.2011.03.053>
- [21] P. J. Olesen, P. J. H. Westerberg and T. Klingberg, "Increased Prefrontal and Parietal Activity after Training of Working Memory," *Nature Neuroscience*, Vol. 7, 2003, pp. 75-79. <http://dx.doi.org/10.1038/nn1165>
- [22] Y. Prabhakaran, K. Narayanan, Z. Zhao and J. D. E. Gabrieli, "Integration of Diverse Information in Working Memory within the Frontal Lobe," *Nature Neuroscience*, Vol. 3, 2000, pp. 85-90. <http://dx.doi.org/10.1038/71156>
- [23] F. Milton, A. J. Wills and T. L. Hodgson, "The Neural Basis of Overall Similarity and Single-Dimension Sorting," *NeuroImage*, Vol. 46, No. 1, 2009, pp. 319-326. <http://dx.doi.org/10.1016/j.neuroimage.2009.01.043>
- [24] M. Neta and P. J. Whalen, "Individual Differences in Neural Activity during a Facial Expression vs. Identity Working Memory Task," *Neuroimage*, Vol. 56, No. 3, 2011, pp. 1685-1692. <http://dx.doi.org/10.1016/j.neuroimage.2011.02.051>
- [25] H. Y. T. Takeuchi, H. Hashizume, Y. Sassa, T. Nagase, R. Nouchi and R. Kawashim, "Failing to Deactivate: The Association between Brain Activity during a Working Memory Task and Creativity," *NeuroImage*, Vol. 55, No. 2, 2011, pp. 681-687. <http://dx.doi.org/10.1016/j.neuroimage.2010.11.052>
- [26] M. A. Thornton and A. R. A. Conwa, "Working Memory for Social Information: Chunking or Domain-Specific Buffer?" *Neuroimage*, Vol. 70, 2013, pp. 233-239. <http://dx.doi.org/10.1016/j.neuroimage.2012.12.063>
- [27] S. Tu, T. H. Li, J. Jou, Q. Zhang, T. Wang, C. Yu and J. Qiu, "An Event-Related Potential Study of Deception to Self Preferences," *Brain Research*, Vol. 1247, 2009, pp. 142-148. <http://dx.doi.org/10.1016/j.brainres.2008.09.090>
- [28] T. P. Zanto, M. T. Rubens, A. Thangavel and A. Gazzale, "Causal Role of the Prefrontal Cortex in Top-Down Modulation of Visual Processing and Working Memory," *Nature Neuroscience*, Vol. 14, 2011, pp. 656-661. <http://dx.doi.org/10.1038/nn.2773>
- [29] T. Hosokawa, K. Kato, M. Inoue and A. Mikam, "Correspondence of Cue Activity to Reward Activity in the Macaque Orbitofrontal Cortex," *Neuroscience Letters*, Vol. 389, No. 3, 2005, pp. 146-151. <http://dx.doi.org/10.1016/j.neulet.2005.07.055>
- [30] E. T. Rolls, H. D. Critchley and J. V. Verhagen, "The Representation of Information about Taste and Odor in the Orbitofrontal Cortex," *Chemosensory Perception*, Vol. 3, No. 1, 2010, pp. 16-33. <http://dx.doi.org/10.1007/s12078-009-9054-4>
- [31] M. Platt and S. A. Huettel, "Risky Business: The Neuroeconomics of Decision Making under Uncertainty," *Nature Neuroscience*, Vol. 11, 2008, pp. 398-403. <http://dx.doi.org/10.1038/nn2062>
- [32] A. Schnider, V. Treyer and A. Buck, "The Human Orbitofrontal Cortex Monitors Outcomes even When No Reward Is at Stake," *Neuropsychologia*, Vol. 43, No. 3, 2005, pp. 316-323. <http://dx.doi.org/10.1016/j.neuropsychologia.2004.07.003>
- [33] Y. K. Takahashi, M. R. Roesch, R. C. Wilson, K. Toreson and P. O'Donnell, "Expectancy-Related Changes in Firing of Dopamine Neurons Depend on Orbitofrontal Cortex," *Nature Neuroscience*, Vol. 14, 2011, pp. 1590-1597. <http://dx.doi.org/10.1038/nn.2957>
- [34] C. M. Ramnani, J. L. Wilson, P. Jezzard, C. S. Carter and S. M. Smith, "Distinct Portions of Anterior Cingulate Cortex and Medial Prefrontal Cortex Are Activated by Reward Processing in Separable Phases of Decision-Making Cognition," *Biological Psychiatry*, Vol. 55, No. 6, 2004, pp. 594-602. <http://dx.doi.org/10.1016/j.biopsycho.2003.11.012>
- [35] M. P. Martin, "Acute Administration of Pregabalin Attenuates Amygdala and Insula During Emotional Face Processing and Anticipation in Healthy Volunteers Biological Psychiatry," *Biological Psychiatry*, Vol. 73, No. 9, 2013, pp. S249-S249.
- [36] R. A. Anderson and H. Cui, "Intention, Action Planning, and Decision Making in Parietal-Frontal Circuits," *Neuron*, Vol. 63, No. 5, 2009, pp. 568-583.
- [37] A. P. Fontana, J. M. Kilner, E. C. Rodrigues, M. Joffily, N. Nighoghossian, C. D. Vargas and A. Sirigu, "Role of the Parietal Cortex in Predicting Incoming Actions," *NeuroImage*, Vol. 59, No. 1, 2012, pp. 556-564. <http://dx.doi.org/10.1016/j.neuroimage.2011.07.046>
- [38] M. D. Hesse, C. M. Thiel, K. E. Stephan and G. R. Fin, "The Left Parietal Cortex and Motor Intention: An Event-Related Functional Magnetic Resonance Imaging Study," *Neuroscience*, Vol. 140, No. 4, 2006, pp. 1209-1221. <http://dx.doi.org/10.1016/j.neuroscience.2006.03.030>
- [39] E. Jefferies, "The Neural Basis of Semantic Cognition: Converging Evidence from Neuropsychology, Neuroimaging and TMS," *Cortex*, Vol. 49, No. 3, 2013, pp. 611-625.
- [40] M. C. Keuken, A. Hardie, B. T. Dorn, S. Dev, M. P. Paulus, K. J. Jonas, W. P. M. Van Den Wildenberg and J. A. Pineda, "The Role of the Left Inferior Frontal Gyrus in Social Perception: An rTMS Study," *Brain Research*, Vol.

- 1383, 2011, pp. 196-205.
<http://dx.doi.org/10.1016/j.brainres.2011.01.073>
- [41] K. Sakai and R. E. Passingham, "Prefrontal Interactions Reflect Future Task Operations," *Nature Neuroscience*, Vol. 6, No. 1, 2002, pp. 75-81.
<http://dx.doi.org/10.1038/nn987>
- [42] S. W. Chang, J. F. Gariépy and M. L. Platt, "Neuronal Reference Frames for Social Decisions in Primate Frontal Cortex," *Nature Neuroscience*, Vol. 16, No. 2, 2010, pp. 243-250. <http://dx.doi.org/10.1038/nn.3287>
- [43] U. Frith and C. D. Frith, "Development and Neurophysiology of Mentalizing," In: C. Frith and D. Wolpert, Eds., *The Neurosciences of Social Interaction*, Oxford University Press, Oxford, 2003, pp. 45-75.
- [44] M. P. Feinstein, D. Leland and A. N. Simmons, "Superior Temporal Gyrus and Insula Provide Response and Outcome-Dependent Information during Assessment and Action Selection in a Decision-Making Situation," *NeuroImage*, Vol. 25, No. 2, 2005, pp. 607-615.
<http://dx.doi.org/10.1016/j.neuroimage.2004.12.055>
- [45] E. T. Rolls and F. Grabenhors, "The Orbitofrontal Cortex and Beyond: From Affect to Decision-Making," *Progress in Neurobiology*, Vol. 86, No. 3, 2008, pp. 216-244.